arXiv:1608.08316v1 [astro-ph.GA] 30 Aug 2016

Toward a Zero-Parameter Model for Galaxy Rotation Curve Data

S. Cisneros[1], J. G. O'Brien[2], N. S. Oblath[1], J. A. Formaggio[1], M. Crowley[3], and K. Mikulski[3]

[1]*Laboratory for Nuclear Science, Massachusetts Institute of Technology, Cambridge, MA 02139, USA*

[2] *Department of Sciences, Wentworth Institute of Technology, Boston, MA 02130, USA*

[3]*Department of Physics, University of Massachusetts Boston, Boston, MA 02125, USA*

Abstract

Modeling the luminous mass components of spiral galaxies in standard gravity poses a challenge due to the missing mass problem. However, with the addition of cold dark matter, the missing mass problem can be circumvented at the cost of additional free parameters to the theory. The Luminous Convolution Model (LCM) reconsiders how we interpret rotation curve data, such that Doppler-shifted spectra measurements can constrain luminous mass discovery. For a sample of 25 galaxies of varying morphologies and sizes, we demonstrate an ansatz for relative galaxy curvatures that can explain the missing mass. We solve for the LCM free parameter, which we report as a ratio of radial densities of the emitter, to receiver galaxy baryonic mass, to an exponent of 1.63. Here, we show that this exponent is sensitive to which Milky Way luminous mass model one chooses. We then make a first prediction regarding the Milky Way mass profile in the inner one kpc. Thus, with a bound on the LCM free parameter, we pave the way for future work, where the LCM will tested as a zero-parameter model to predict luminous mass from rotation curve data.

1

Light from spiral galaxies is considered by two different observational techniques. The first, photometry, is a measure of total luminosity in specific wavelength bands used to trace mass fractions (specific star populations, gas fractions, dust, etc.). From the photometry, mass is associated with total light by population synthesis modeling (PSM). PSM is under-constrained (Conroy *et al.*, 2009) precisely because the second observation of light, Doppler-shifted spectra, yielded the dark matter problem.

PSM returns mass-to-light ratios (M/L) for galaxies, based on a complex suite of model-based assumptions regarding chemical composition, evolution, dust, gas fractions, metallicity, etc. Finding a M/L ratio relies upon distance estimates, based on underconstrained standard candles. The M/L for a given galaxy parametrizes enclosed mass as a function of radius, which then gives test particle motion by the Poisson equation. Resulting rotation curves are the expected Keplerian, declining velocities $v_{lum}(r)$ seen in Fig. (3).

The conflicting observation, Doppler-shifted spectra of characteristic atomic transitions, is interpreted in the Lorentz framework as a relative velocity between frames. The resulting velocity parameter v_{obs} can be seen to be essentially constant at large radii, beyond all stars (Fig. 3). The divergence of the velocities implied by shifted spectra and photometry gave rise to the dark matter problem in spiral galaxies, discovered by Rubin *et al.* (1978) and Bosma (1978). The mismatch between dynamical mass and the luminous mass is generally explained by a class of cold, dark matter halo models (Navarro *et al.*, 1997). There have been successful attempts to test alternate theories such as Modified Newtonian Dynamics (MOND) (Milgrom, 1983) and Conformal Gravity (Mannheim and O'Brien, 2012). Since dark matter halo models have two free parameters, they do little to constrain population synthesis models at the present time (Conroy *et al.*, 2009), and hence serve as a possible interpretation, not as a prediction.

Soon after the discovery of the flat-rotation curve problem, another curious trend was noted by Rubin *et al.* (1980). In Persic *et al.* (1996), it was shown with exquisite precision—in a sample of 1,100 galaxies—that rotation curves fall into a spectrum inflected about the Milky Way's rotation curve. This spectrum is known as the Universal Rotation Curve (URC); it is interpreted that galaxies smaller than the Milky Way are dark matter dominated, and those larger require only minimal dark matter halos.

As dark matter particles are hypothesized to interact in the standard gravitational manner, there exists no physical reason for smaller galaxies to accrete dark matter halos more successfully than larger galaxies. Likewise, the unexplained position of the Milky Way in the middle of the URC spectrum is suggestive. Thus, we instead interpret the URC as indicative of frame-dependent effects due to our observing frame, the Milky Way Galaxy, in the heuristic construction of the

Luminous Convolution Model (LCM). This will serve as the starting point for the LCM interaction, and we show that the URC spectrum can be explained compactly based on this model prescription.

The LCM is a fitting prescription, with one free parameter b, which we show in this work can be reduced to a constant dependent on the specific choice of the Milky Way luminous mass model. The LCM ansatz is that the relative, very small gravitational curvatures of very large frames are convolved in our observations of shifted spectra. This statement is reminiscent of the MOND paradigm (Milgrom, 1983), though it exploits changing relative curvatures (LCM) as opposed to modified accelerations (MOND).

Usually, relative galaxy curvature effects are ignored in the flat-rotation curve problem, as they are about four orders of magnitude smaller than the relative velocity effects when phrased kinematically. Commonly, relative curvature effects are evaluated (and obviated) by taking the algebraic difference of the gravitational redshifts of a galaxy from those of the Milky Way (Misner *et al.*, 1970). This is a Galilean transformation of frames, and the photon wave-vector should instead transform within the Lorentz group. Hence, we instead use photon redshift frequencies to define relative galaxy frames, related through the Lorentz boost architecture to quantify the relationship kinematically. Kinematic phrasing of gravitational redshifts is common in astrophysics, what is new is the treatment of *relative* curvatures.

In this paper, the chosen sample of 25 galaxies is selected in an effort to represent a full spectrum of galaxy sizes and morphologies, and no other bias was placed on selection. This sample was used to both identify the LCM free parameter and constrain the Milky Way luminous mass model. We propose that when the LCM reproduces rotation curve data perfectly, as is the case in the current sample, that the resulting luminous mass profiles demonstrate agreement between the two observations of Dopper-shifted spectra and photometry. Hence, the LCM introduces a constraint to luminous mass modeling directly from Doppler-shifted spectra, using luminous matter estimates within the range defined by photometry. By considering the small frame effects due to relative curvatures of spiral galaxies, the LCM is a successful fitting formula which offers a simple explanation for the URC spectrum based on luminous mass estimates.

This paper is organized as follows: Sec. 2 sketches the heuristic construction of the LCM fitting formula, Sec. 3 describes the fitting method, Sec. 4 offers analysis of the results, and Sec. 5 details conclusions and future directions.

2 LCM fitting formula

Dark matter (DM) theories interpret the discrepancy between rotation curve data and Keplerian photometry predictions as the missing mass problem. The dark mass is hypothesized to interact only gravitationally with ordinary baryonic matter. This assumption is treated with the rotation curve for-

mula,

$$v_{rot}^2 = v_{lum}^2 + v_{dark}^2, \quad (1)$$

where the prediction v_{rot} is fitted to reported rotation curve velocity data (v_{obs} from shifted spectra ω'). The term v_{dark} is the contribution to rotation due to a spherically symmetric dark matter halo, and v_{lum} is from the baryonic contribution. The rotation curve formula is a mass sum $M_{dynamical} = M_{lum} + M_{dark}$, as terms in v^2 represent centripetal accelerations due to enclosed mass as a function of radius. The functional forms of the terms in Eq. (1) have been well-established (Mannheim (2006)) and usually provide an accurate statistical fit to the data due to the presence of two free parameters per galaxy in v_{dark}.

2.1 LCM construction

The LCM modifies Eq. (1), by replacing the DM halo velocity contributions, v_{dark}^2, with the relative curvature convolution, $\tilde{v}_{lcm}^2$, in the fitting formula:

$$v_{rot}^2 = v_{lum}^2 + \alpha \tilde{v}_{lcm}^2, \quad (2)$$

where α is a dimensionless fitting parameter and $\tilde{v}_{lcm}^2$is a function of luminous mass only.

We find in this work (see Fig. 2) that the free parameter is correlated with the dimensionless ratio,

$$\alpha = \left(\frac{\rho_{mw}}{\rho_{gal}}\right)^b. \quad (3)$$

The subscript mw indicates the galaxy receiving the photon and the subscript gal indicates the photon emitting galaxy. Radial densities ρ_{mw} and ρ_{gal} are defined by:

$$\rho_r = \frac{M_{total}}{r_e}, \quad (4)$$

where the total integrated luminous mass at the limit of the photometric data is M_{total}, and r_e is the exponential galactic disk scale length from fitting the resulting LCM luminous mass profile with the standard form of the galactic thin disk. Hence, for a given choice of the MW we can establish the free parameter space and fit for the exponent b, as shown in Fig. 2. We report for a given Milky Way the exponent b appears to be a constant.

The LCM mapping $\tilde{v}_{lcm}^2$ is a convolution of two Lorentz-type transforms v_1 and v_2:

$$\tilde{v}_{lcm}^2 = \kappa^2 v_1 v_2, \quad (5)$$

scaled by a curvature ratio κ,

$$\kappa(r) = \frac{c - \tilde{c}_{gal}(r)}{c - \tilde{c}_{mw}(r)}. \quad (6)$$

Coordinate light speeds $\tilde{c}_{gal}(r)$ and $\tilde{c}_{mw}(r)$ are defined by the pseudo-index of refraction $n(r)$ (Narayan *et al.*, 1997),

$$n(r)\tilde{c}_{frame} = \left(\frac{1}{\sqrt{-g_{tt(r)}}}\right)_r \tilde{c}_{frame} = c. \quad (7)$$

and represent deviations from flatness for some mass distribution which is symmetric about a central value of $r = 0$. The term g_{tt} is defined as the Schwarzschild time metric coefficient.

The term v_1 is the relative galaxy-to-galaxy transform. It is based on comparing the standard frequency form of the Lorentz Doppler shift formula to its hyperbolic form,

$$\frac{v_{obs}(r)}{c} = \frac{\frac{\omega'(r)}{\omega_o} - \frac{\omega_o}{\omega'(r)}}{\frac{\omega'(r)}{\omega_o} + \frac{\omega_o}{\omega'(r)}} = \frac{e^{\xi} - e^{-\xi}}{e^{\xi} + e^{-\xi}} \tag{8}$$

and identifying the Lorentz boost exponential e^{ξ} with the frequencies sent and received, respectively ω_o and ω'.

We define slightly curved galaxy manifolds by the Schwarzschild gravitational redshift frequencies $\omega(r)$

$$\frac{\omega_o}{\omega(r)} = \left(\frac{1}{\sqrt{-g_{tt}}}\right)_r, \tag{9}$$

where ω_o is the characteristic photon frequency.

We use the the weak field form of the time metric coefficient g_{tt} (Hartle, 2003)

$$g_{tt}(r) \approx -1 + 2\frac{\Phi(r)}{c^2}, \tag{10}$$

where Φ is the Newtonian scalar gravitational potential defined by the luminous mass reported from photometry.

In Special Relativity, the two frames involved in Lorentz transformation are perfectly symmetric, so there is no distinction between who is the emitter and who is the receiver of the photon. However, as we transition to slightly curved galaxy frames, we pin the Lorentz frames with redshift frequencies emitted and received

$$e^{\xi} = \frac{\omega'_{receiver}}{\omega_{emitter}}, \tag{11}$$

for consistency. It is common practice to use the functional form in Eq. 8 to rephrase gravitational redshifts kinematically (Cisneros *et al.* (2015); Radosz *et al.* (2013)).

So, the term v_1 is based on the Lorentz exponential term:

$$e^{\xi_c}(r) = \frac{\omega_{mw}(r)}{\omega_{gal}(r)}. \tag{12}$$

Here ω_{mw} and ω_{gal}, are compared one-to-one in radii, and are the gravitational redshifts for mw the receiving galaxy (MW) and gal the photon emitting galaxy. It is this pseudo-rapidity angle ξ_c which explains trends in the Universal Rotation Curve of Persic *et al.* (1996).

The transformation v_1 is

$$\frac{v_1}{c} = \left(\frac{1}{\cosh \xi_c} - 1\right) = \left(\frac{2}{e^{\xi_c} + e^{-\xi_c}} - 1\right). \tag{13}$$

which can be interpreted as the difference from unity of the coordinate time of the galaxy emitting the photons with respect to the proper time of the Milky Way.

The second transformation, v_2, is a Lorentz boost which transforms between the curved 2-frame ξ_c (Eq. 12) to the flat 2-frame where observations are made. By the constancy of the speed of light, it is evident that observations are always made in flat-frames. The term e^{ξ_f} defines the flat-frames involved in our observations, and is defined by ω_l, the expected frequency shifts for Keplerian orbital velocities predicted from photometry:

$$e^{\xi_f}(r) = \frac{\omega_l(r)}{\omega_o}. \tag{14}$$

Keplerian rotations are our best estimates of what would be observed in the absence of relative curvature effects, as evidenced by the Solar System orbital velocity profiles which do not require dark matter.

According to the convention established in Eq. 11, the Lorentz mapping term is defined by the curved 2-frame into flat 2-frame

$$(e^{\xi_2})^2 = \frac{e^{\xi_f}}{e^{\xi_c}}. \tag{15}$$

The term e^{ξ_c} is defined as per Eq. 12.

The transformation v_2—found to be the most robust across the sample—is the a ratio of the hyperbolic Lorentz boost evaluated at the limit of the data, v_τ, to the same boost at each radii, $v(r)$,

$$v_2 = \frac{v_\tau}{v(r)}. \tag{16}$$

The value at the limit of the data v_τ is a good approximation of the final extent of the baryon profile. The form of the hyperbolic boost is

$$\frac{v(r)}{c} = \tanh \xi_2 = \frac{(e^{\xi_2})^2 - 1}{(e^{\xi_2})^2 + 1}. \tag{17}$$

3 Method

The LCM rotation curve velocity prediction, v_{rot} (Eq.2), is fit to reported rotation curve data v_{obs}, and the ξ^2 is minimized to best match the luminous mass profile to the v_{obs} data. We use the MINUIT minimization software as implemented in the ROOT data-analysis package (Brun and Rademakers, 1997), as follows:

1. A database of modern estimates of the luminous mass components (gas, disk, bulge) are collected from the cited references.

2. The associated Newtonian gravitational potential Φ is calculated for each component and summed by superposition to parametrize Eq. 10;

3. The convolution function, v_{lcm}, is calculated using a choice of the Milky Way luminous mass profile;

4. The fit is performed, and the procedure iterated to find the optimal luminous profile (v_{obs}) which best reflects the rotation curve data (v_{rot});

5. the value for the LCM free parameter α is recorded and added to our parameter space to constrain the ansatz in Eq. 3.

By iterating the luminous mass within bounds imposed by photometry, we reproduce rotation curve data almost exactly (see Fig. 3). The fits and resulting free parameter space reported here represent this LCM prescription.

4 Discussion & Analysis

4.1 A constraint to the Milky Way and the LCM free parameter

The LCM is sensitive to both the emitter and receiver galaxies, so the choice of input Milky

Way data is essential. Since we make observations from within the system, the Milky Way luminous mass profile is notoriously difficult to determine (Carignan and Chemin, 2006). We have compared each of the 25 galaxies in our sample to (4) different, well studied Milky Way (MW) luminous mass models; Sofue (2013), Xue *et al.* (2008), and two models from Klypin *et al.* (2002). Table 1 and Fig. 1 compare the salient features of the MW models.

The sample of 25 galaxies reported here encompasses a large variation in estimication of the common physical trends in the free parameter space. The complete set of individual emitter galaxy results are reported in Cisneros *et al.* (2015), and include α, M/L, r_e, the LCM reduced χ^2, the reduced χ^2 values for the DM or alternative gravity model which were originally used to fit to the same data in the cited texts. The LCM luminous mass results for the 25 galaxies are consistent with documented bounds from photometry (de Blok *et al.*, 2008).

In Fig. 2, we show the α free parameter space for each MW model. Each dot in the figures represents one galaxy α fit result, against thet specified MW. To test the correlation of α with the ansatz $\alpha = (\rho_1/\rho_2)^b$, in Eq. 3, we fit the luminous profiles which result in each LCM fit with a thin disk, and use the resulting fit value of the scale length r_e and an integrated total mass M to parametrize $\rho = M/r_e$. This process also gives the mass to light ratio (M/L) reported previously (Cisneros *et al.*, 2015), using modern reports of the distance and luminosities L (see Fig. 2). Plots of the α distribution versus the guess $\alpha = (\rho_1/\rho_2)^b$ for each MW choice are shown in in Fig. 2. The exponent b found for each MW choice appears to be constant. Interesting, but beyond the scope of the current work, is that the b exponents for the MW models in our sample are very similar to the exponents commonlly reported for dark matter halo density profiles (Navarro *et al.*, 1997). Iin a future blind study the LCM free parameter α will be tested as a constant for a given MW choice against a new sample. Currently, the most robust MW model by far across the current sample is the Sofue (2013) MW, which has an associated value of $b = 1.64 \pm 0.03$.

The Sofue (2013) MW model is by far the most centrally peaked velocity profile within the first kpc. This is an LCM prediction which can be falsified when the Large Event Horizon () tightens the photometric constraints on this region of our galaxy.

We find that the MW models in our sample which are less centrally dense can not fit the bulge dominated galaxies such as NGC 2841, NGC 7814, NGC 7331 and NGC 5055 without artificial bounding on the model's free parameter. Even when bounding is imposed artificially in the fitting process, the remain very centrally dense galaxies such as NGC 7814 which can only be fit using the Sofue MW. Fits using the less centrally dense MW models fail completely for this galaxy. In fact, it is the sensitivity to MW choice for these type of galaxy which allows degeneracy breaking of our central MW baryon gradient. In this paper, all rotation curve figures reflect the hybrid MW choice of the Sofue stellar bulge, and the Xue *et al.* (2008) stellar

disk. The Xue stellar disk is used due to it's high radial extent which allows LCM galaxy fits out to 60 kpc in reported rotation curve data. The stellar disks of all four MW model reported here are asymptotically very similar.

It is also interesting to note that the two galaxies NGC 891 and NGC 7814 from Fraternali *et al.* (2011) in can be compared as an example of galaxies with very similar enclosed mass at the limit of the data, but very different distributions of that mass. In Fig. 3, it is clear that the slope of the relative curvature contributions for these two galaxy reflect the different density gradients. The ultasensitivity of NGC 7814 to small changes in the input luminous mass profile (within a tolerance of $\pm$10s of m/sec) is not mimicked by the NGC 891 fits, which is robust to a range of MW choices. We believe the sensitivity of NGC 7814 fits, and for similar galaxies, is due to when a galaxy being observed is very similar to the curvature of our own MW in some region. For NGC 7814, that region is the central one kpc.

4.2 Universal Rotation Curve trends

The galaxy-to-galaxy pseudo rapidity angle ξ_c (Eq. 12) gives a simple explanation for the Universal Rotation Curve distribution (Persic *et al.*, 1996). As can be seen in Fig. 4, the inflection of the reported rotation curves at high radii is mirrored by the $\xi_c(r)$ function in the galaxy disk. The term,

$$\xi_c(r) = \ln\left(\frac{\omega_{mw}(r)}{\omega_{gal}(r)}\right). \qquad (18)$$

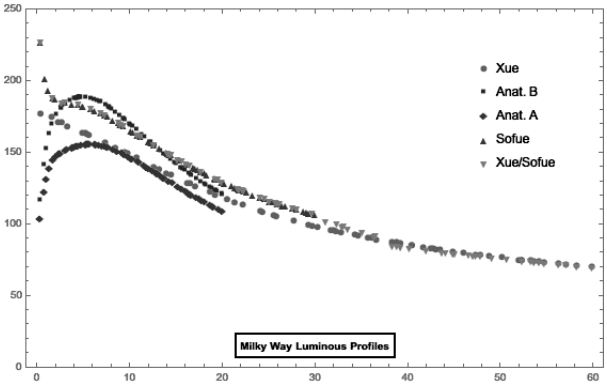

Figure 1: Milky Way Luminous mass models tested for the LCM mapping construction, reported in terms of orbital velocities (km/sec) as a function of radius (kpc).

is a map of the galaxy being observed onto our own Milkky Way, one-to-one in radius.

In terms of the gravitational redshifts,

$$\xi_c = \ln\left(\frac{\sqrt{-g_{tt,mw}(r)}}{\sqrt{-g_{tt,gal}(r)}}\right) = \frac{1}{2}\ln\left(\frac{g_{tt,mw}(r)}{g_{tt,gal}(r)}\right). \qquad (19)$$

In current analysis of the sample, all galaxy pseudo-rapidity angles tend to a constant, non-zero value at high radius, on the order of 10^{-6}, and appear to act as envelope functions to the rotation curves observed.

5 Conclusions

In this paper we show how the LCM fitting formula can reconcile observations of Doppler-shifted spectra and photometry by the inclusion of relative galaxy curvatures. Relative curvature imposes the importance of the choice of a Milky Way luminous mass

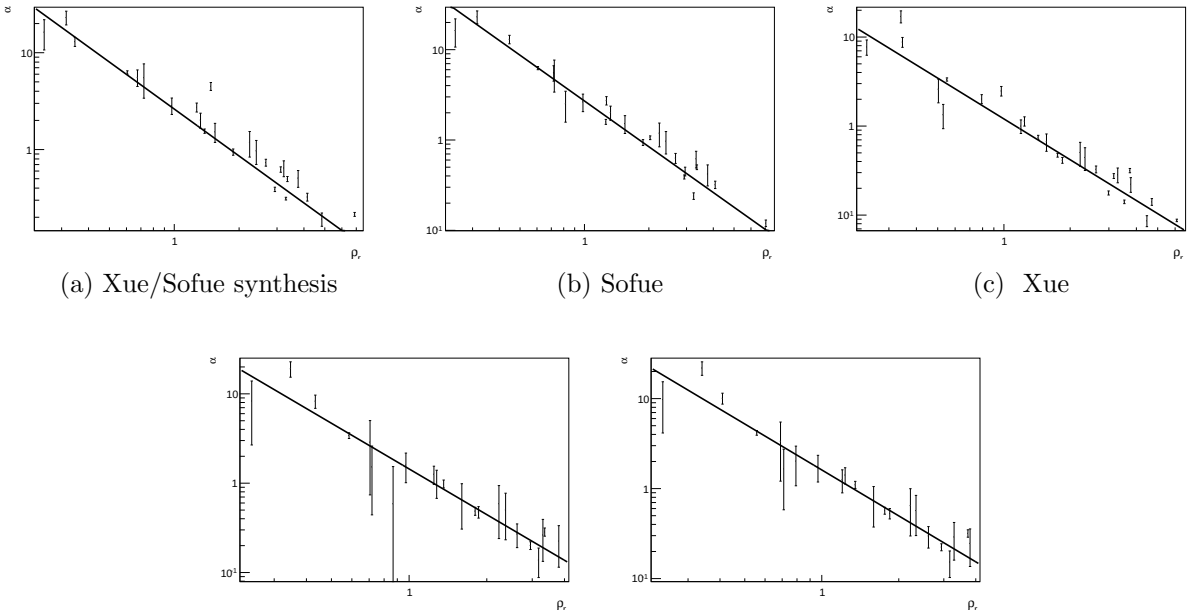

(a) Xue/Sofue synthesis (b) Sofue (c) Xue

(d) Klypin model A (e) Klypin model B

Figure 2: Log-log plot of LCM free parameter, α, versus the guess at a physical interpretationin in Eq. 3 . Each dot represents one of the galaxies in the sample, for each Milky Way model. Errors are statistical only. Some Milky Way models did not return LCM fits for each galaxy in the sample.

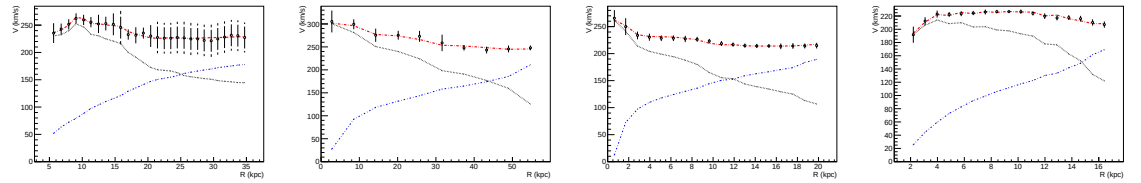

(a) M 31, Ref. 7 (b) NGC 5533, Ref. 5 (c) NGC 7814, Ref. 6 (d) NGC 891, Ref. 6

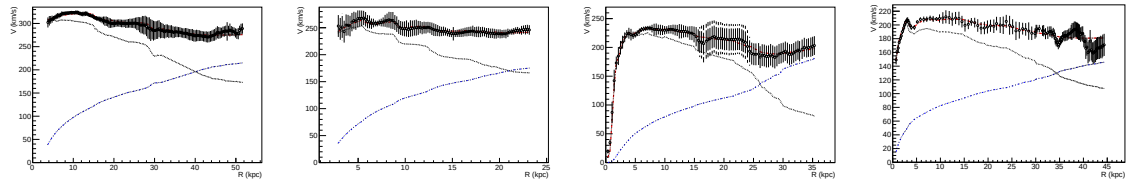

(e) NGC 2841, Ref. 4 (f) NGC 7331, Ref. 4 (g) NGC 3521, Ref. 4 (h) NGC 5055, Ref. 2

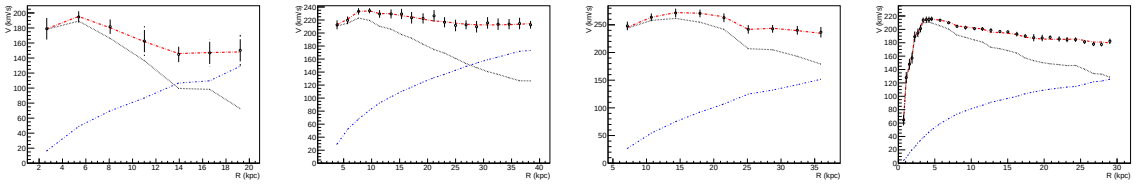

(i) NGC 4138, Ref. 5 (j) NGC 5907, Ref. 5 (k) NGC 3992, Ref. 5 (l) NGC 2903, Ref. 5

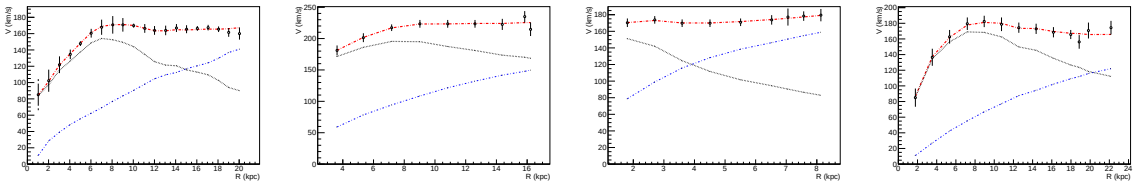

(m) NGC 6946, Ref. 5 (n) NGC 3953, Ref. 5 (o) UGC 6973, Ref. 5 (p) NGC 4088, Ref. 5

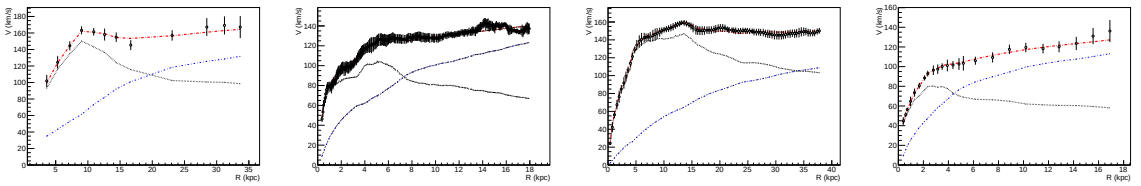

(q) NGC 3726, Ref. 5 (r) NGC 2403, Ref. 2 (s) NGC 3198, Ref. 2 (t) M 33, Ref. 3

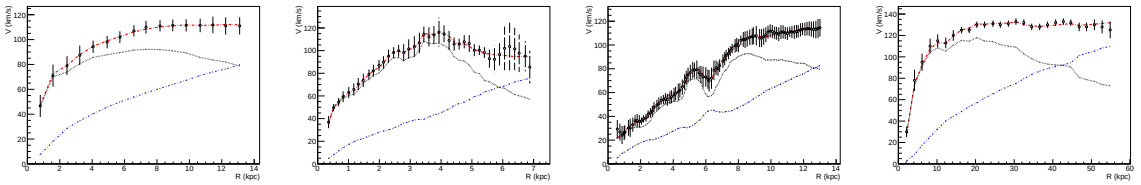

(u) F 563-1, Ref. 1 (v) NGC 7793, Ref. 8 (w) NGC 925, Ref. 2 (x) UGC 128, Ref. 4

Figure 3: Circles with associated error bars are reported rotation curve data, red dotted-dash lines are LCM fits, blue dotted-dash line are relative curvature, and black dotted line are luminous mass results. All fits shown are in comparison to the Sofue (2013); Xue *et al.* (2008)

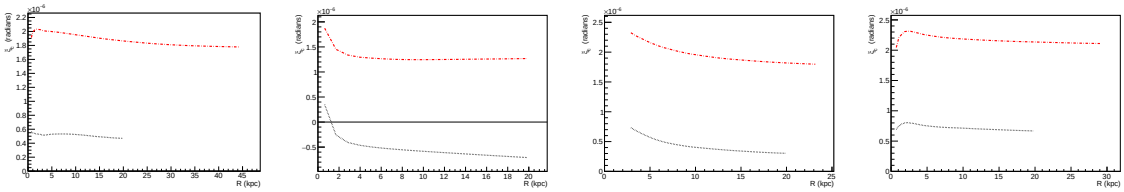

(a) NGC 5055, ξ_c (b) NGC 7814, ξ_c (c) NGC 7331, ξ_c (d) NGC 2903, ξ_c

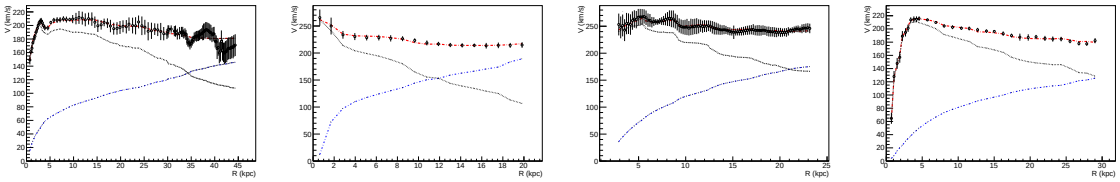

(e) NGC 5055 (f) NGC 7814 (g) NGC 7331 (h) NGC 2903

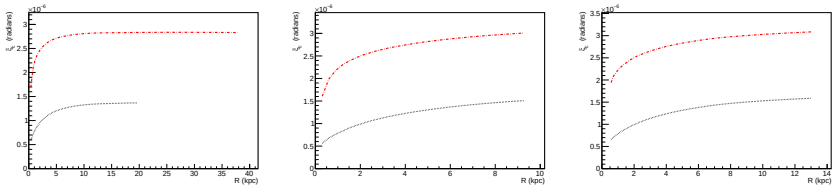

(i) NGC 3198, ξ_c (j) UGC 7524 , ξ_c (k) NGC 925, ξ_c

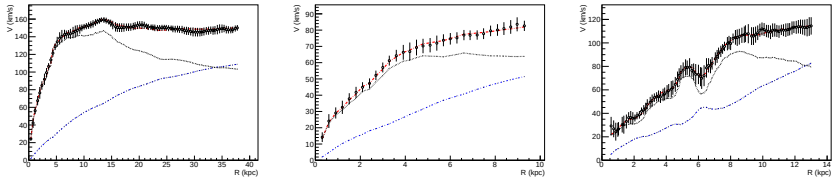

(l) NGC 3198 (m) UGC 7524 (n) NGC 925

Figure 4: Universal Rotation Curve comparison: graphs of the Galaxy psuedo-rapidity angle (radians) as a function of radius (kpc) in figures (a)-(d) and (i)-(k), red dotted lines are for the MW choice from Sofue (2013) and Xue *et al.* (2008), and black dotted lines from Klypin *et al.* (2002) Model B. Rotation curves (km/s vs. kpc) are presented under corresponding galaxy ξ_c pictures, and lines and galaxy references are as in Fig. 3.

Table 1: Milky Way Luminous Mass Model results

Galaxy	R_{last}	M_{bulge}	M_{disk}	b	r_e	χ^2_R	dof
Xue/Sofue	60	1.8	5.30	1.61	3.74	13.19	24
Sofue	30	1.8	6.80	1.68	4.76	6.52	23
Xue	60	1.5	5.00	1.52	5.76	11.45	24
Klypin, A	15	0.8	4.00	1.70	3.87	1.76	20
Klypin, B	15	1.0	5.00	1.70	4.53	2.65	20

Table 2: Exponent b for the LCM free parameter $\alpha = (\rho_{mw}/\rho_{gal})^b$, solved for by power law fits to the distributions in Fig. 2. Integrated mass for the bulge M_{bulge} and disk M_{disk} are in units of $10^{10} M_\odot$), and exponential scale lengths r_e are in kpc. R_{last} is the limit of the reported Milky Way luminous mass model in kpc.

model, and we report our findings in this paper as to what we consider the most physical Milky Way model. With the unprecedented observational resolution of the Large Event Horizon telescope this portion of the LCM prediction can be falsified, and could further provide a constraint to our understanding of our Milky Way. The fitting formula presented in this paper is a first approach to a zero-parameter model in galaxy rotation curve modeling. We have shown the free parameter can be reduced to a constant value for a given choice of a Milky Way luminous mass profile.

Further, we have also shown that the LCM fitting formula can provide an alternate explanation to the Universal Rotation Curve groupings of Persic *et al.* (1996), based only on estimates of luminous mass. As can be seen in Fig. 3, the luminous profiles used to fit the rotation curves are well within physical bounds implied by photometry.

Although this is an attempt to explain rotation curves in a zero-parameter setting, any alternative gravitational model must be able to account for other phenomena currently attributed to cold dark matter. Thus, in future work, the LCM must address questions of weak lensing, galaxy mergers, clusters of galaxies and early structure formation. However, none of these problems can be investigated until there is an agreed upon estimate for the baryon distribution in the Local Group of galaxies. An equally interesting future question is how to phrase an LCM-style conjecture for the rotation curve of the Milky Way itself. Since we are within the emitter frame it will involve a map where the observer's frame is embedded in the emitter's global frame. The phenomenolgical implications of this question could provide testing much later in the future, since this prescription could be made for any emitter-receiver galaxy pair, and hence provide predictions for

how rotation curves could be viewed from any arbitrary frame.

5.1 Acknowledgments

The authors would like to thank V. P. Nair, P. Schechter, R. A. M. Walterbos, T. Boyer, P. Fisher, R. Ott, K. Chng, and S. Rubin. J. A. Formaggio and N. A. Oblath are supported by the United States Department of Energy under Grant No. DE-FG02-06ER-41420.

References

Bosma, A. (1978). *The distribution and kinematics of neutral hydrogen in spiral galaxies of various morphological types*. Ph.D. thesis, PhD Thesis, Groningen Univ., (1978).

Brun, R. and Rademakers, F. (1997). Root. *Nucl. Inst. & Meth. in Phys. Res. A*, **389**, 81–86.

Carignan, C. and Chemin, L. (2006). Extended hi rotation curve and mass distribution of m31. *ApJ*, **641**, L109–L112.

Cisneros, S., Goedecke, G., Beetle, C., and Engelhardt, M. (2015). On the Doppler effect for light from orbiting sources in Kerr-type metrics. *Mon.Not.Roy.Astron.Soc.*, **448**, 2733–2736.

Cisneros, S., O'Brien, J. G., Oblath, N. S., and Formaggio, J. A. (2015). The Luminous Convolution Model for spiral galaxy rotation curves. *ArXiv e-prints*.

Conroy, C., Gunn, J., and White, M. (2009). The propagation of uncertainties in stellar population synthesis modeling i: The relevance of uncertain aspects of stellar evolution and the imf to the derived physical properties of galaxies. *ApJ*, **699**, 486.

Corbelli, E. (2003). Dark matter and visible baryons in m33. *MNRAS*, **342**, 199.

de Blok, W., Walter, F., , and Brinks, E. (2008). High-resolution rotation curves and galaxy mass models from things. *AJ*, **136**, 2648.

Dicaire, I., Carignan, C., Amram, P., Marcelin, M., Hlavacek-Larrondo, J., *et al.* (2008). Deep fabry-perot halpha observations of ngc 7793: a very extended halpha disk and a truly declining rotation curve. *AJ*, **135**.

Fraternali, F., Sancisi, R., , and Kamphuis, P. (2011). A tale of two galaxies, light and mass ngc 891 and ngc 7814. *A&A*, **http://arxiv.org/abs/1105.3867**.

Hartle, J. (2003). *Gravity*. Addison-Wesley.

Klypin, A., Zhao, H., and Somerville, R. (2002). Extended hi rotation curve and mass distribution of m31. *ApJ*, **573**, 597.

Mannheim, P. D. (2006). Alternatives to dark matter and dark energy. *Progress in Particle and Nuclear Physics*, **56**, 340–445.

Mannheim, P. D. and O'Brien, J. G. (2012). Fitting galactic rotation curves with conformal gravity and a global quadratic potential. *Phys. Rev. D*, **85**, 124020.

Mannheim, P. D. and O'Brien, J. G. (2013). Galactic rotation curves in conformal gravity. *Journal of Physics Conference Series*, **437**(1), 012002.

Milgrom, M. (1983). A modification of the newtonian dynamics- implications for galaxies. *ApJ*, **270**, 371.

Misner, C., Thorne, K., and Wheeler, J. (1970). *Gravitation*. W.H. Freeman and Company, New York, NY, USA.

Narayan, R., , and Bartelman, M. (1997). *Formation of Structure in the Universe: Lectures on Gravitational Lensing*. A. Dekel & J. P. Ostriker.

Navarro, J. (1998). The Cosmological Significance of Disk Galaxy Rotation Curves. *arxiv:astro-ph/9807084* .

Navarro, J., Frenk, C., and White, S. (1997). The structure of cold dark matter halos. *ApJ*, **462**, 563.

Persic, M., Salucci, P., and Stel, F. (1996). The universal rotation curve of spiral galaxies - I. The dark matter connection. *MNRAS*, **281**, 27–47.

Radosz, A., Augousti, A. T., and Siwek, A. (2013). On the nature of cosmological redshift and spectral shift in Schwarzschild-like and other spacetimes. *Gen.Rel.Grav.*, **45**, 705–715.

Rubin, V., Ford, W., and Thonnard, N. (1980). Rotational properties of 21 sc galaxies with a large range of luminosities and radii. *ApJ*, **238**, 471.

Rubin, V. C., Thonnard, N., and Ford, Jr., W. K. (1978). Extended rotation curves of high-luminosity spiral galaxies. IV - Systematic dynamical properties, SA through SC. *ApJ*, **225**, L107–L111.

Sanders, R. and McGaugh, S. (2002). Modified newtonian dynamics as an alternative to dark matter. *ARA&A*, **40**, 263.

Sofue, Y. (2013). *Mass Distribution and Rotation Curve in the Galaxy*, page 985. Oswalt, T. D. and Gilmore, G.

Xue, X. *et al.* (2008). The Milky Way's Circular Velocity Curve to 60 kpc and an Estimate of the Dark Matter Halo Mass from Kinematics of 2400 SDSS Blue Horizontal Branch Stars. *AJ.*, **684**, 1143–1158.